TABLE 1. Summary of Patients

Age	Sex	Defect Etiology	Defect Size (cm)	Complication
17	F	Burn contracture	4.1 × 2.2	Partial necrosis
18	F	Tumor resection	5.8 × 3.9	–
52	M	Cutaneous fistula exicion	3.8 × 3	–
45	M	Tumor resection	4.2 × 3.1	–
50	M	Tumor resection	4.7 × 2.9	–
30	F	Congenital nevus exicion	4.5 × 3.5	–

the dissection, especially in the tunnel around the pedicle to prevent hematoma and squeeze the pedicle.

Even though the submental artery flap can be used as a fasica-cutaneous or cutaneous flap, some authors recommend inclusion of the ipsilateral digastric muscle to prevent problems in venous drainage because the pedicle passes deep to the digastric muscle in 70% of the patients. However, according to the study by Martin et al,[5] all flaps that were prepared without inclusion of the digastric muscle survived. We also did not include the digastric muscle into the flap, and thus obtained a thinner and more pliable flap that improved the aesthetic outcomes (Table 1).

CONCLUSION

The submental artery perforator island flap is a useful option for reconstruction of middle-sized defects. The decision to include the anterior digastric muscle into the flap is made according to the size, location, and nature of the defect. Including the digastric muscle makes the flap more thick and bulky. In defects that require a thin flap, the anterior digastric muscle may not be included, thus providing more aesthetic and functional results.

Although we prefer the free tissue transfer for large-sized defects, the submental artery perforator island flap without inclusion of the digastric muscle is a reliable and suitable option for the medium-sized defects in the lower face and intraoral defects.

REFERENCES

1. Moschella F, Cordova A. Depressor flaps for large defects of the lower lip and mental region. *Plast Reconstr Surg* 2005;115:252
2. Bayramicli M, Numanoglu A, Tezel E. The mental V-Y island advancement flap in functional lower lip reconstruction. *Plast Reconstr Surg* 1997;100:1682
3. Shi CL, Wang XC. Reconstruction of lower face defect or deformity withy submental artery perforator flaps. *Ann Plast Surg* 2012;69:41–44
4. Martin D, Baudet J, Mondie JM, et al. The submental island skin flap: a surgical protocol. Prospects of use. *Ann Chir Plast Esthet* 1990;35:480
5. Martin D, Pascal JF, Baudet J, et al. The submental island flap: a new donor site. Anatomy and clinical applications as a free or pedicled flap. *Plast Reconstr Surg* 1993;92:867
6. Jiang GH, Yan JH, Lin CL, et al. Anatomic study of the facial artery using multislice spiral CT angiography. *Nan Fang Yi Ke Da Xue Xue Bao* 2008;28:457e459
7. Curran AJ, Neligan P, Gullane PJ. Submental artery island flap. *Laryngoscope* 1997;107:1545–1549
8. Sterne GD, Januszkiewicz JS, Hall PN, et al. The submental island flap. *Br J Plast Surg* 1996;49:85–89
9. Faltaous AA, Yetman JR. The submental artery flap: an anatomic study. *Plast Reconst Surg* 1996;97:56–60
10. Parmar PS, Goldstein DP. The submental island flap in head and neck reconstruction. *Curr Opin Otolaryngol Head Neck Surg* 2009;17:263–266
11. You YH, Chen WL, Wang YP, et al. Reverse facial-submental artery island flap for the reconstruction of maxillary defects after cancer ablation. *J Craniofac Surg* 2009;20:2217–2220
12. Zhang CC, Wang JG, Yue ZL, et al. Clinical study of submental artery island myocutaneous flap for reconstruction of oral and maxillofacial defects following operation. *Chin J Otorhinolaryngol Head Neck Surg* 2012;47:285–288
13. Rahpeyma A, Khajehahmadi S. Submental artery island flap in intraoral reconstruction: a review. *J Craniomaxillofac Surg* 2014;42:983–989
14. Hwang K, Han JY, Chung RS, et al. Submental perforating artery: a culprit of bleeding during facelift. *J Craniofac Surg* 2005;16:3e5
15. Akan IM, Özdemir R, Uysal A, et al. The submental artery flap. *Eur J Plast Surg* 2001;24:134–139
16. Saleh DB, Fourie LR, Mizen KD. The extended sub-mental artery flap for complex orofacial reconstruction. *Plast Reconst Surg* 2012;130:5S–1
17. Martin D. The super extended sub-mental flap or combo sub-mental flap. *Ann Chir Plast Esthét* 2014;59:294–297
18. Pistre V, Pelissier P, Martin D, et al. Ten years of experience with the submental flap. *Plast Reconst Surg* 2001;108:1576–81
19. Martin D, Pascal JF, Baudet J, et al. The submental island flap: a new donor site. Anatomy and clinical applications as a free or pedicled flap. *Plast Reconstr Surg* 1993;92:867–73
20. Chen WL, Li JS, Yang ZH, et al. Two submental island flaps for reconstructing oral and maxillofacial defects following cancer ablation. *J Oral Maxillofac Surg* 2008;66:1145–56
21. Sagüillo K, García-Serrano G, Almeida F, et al. Submental flap in reconstruction of orofacial defects. *Revista Española Cirugía Oral Maxilofacial (English Edition)* 2015;37:196–201
22. Hurwitz DJ, Rabson JA, Futrell JW. The anatomic basis for the platysma skin flap. *Plast Reconstr Surg* 1983;72:302–314
23. Chen HC, Liu CJ. Full reconstruction of a maxillary hard palate defect using a retrograde submental island flap in an adenoid cystic carcinoma: a case study. *J Oral Maxillofac Surg Med Pathol* 2015;27:348–352
24. Kim JT, Kim SK, Koshima I, et al. An anatomic study and clinical applications of the reversed submental perforator-based island flap. *Plast Reconstr Surg* 2002;109:2204–2210
25. Varghese BT. Optimal design of a submental artery island flap. *J Plast Reconstr Aesthet Surg* 2011;64:e183–e184
26. Parmar PS, Goldstein DP. The submental island flap in head and neck reconstruction. *Curr Opin Otolaryngol Head Neck Surg* 2009;17:263–266
27. Zhang B, Wang JG, Chen WL, et al. Reverse facial-submental artery island flap for reconstruction of oropharyngeal defects following middle and advanced-stage carcinoma ablation. *Br J Oral Maxillofac Surg* 2011;49:194e197
28. Rojananin S, Igarashi T, Ratanavichitrasin A, et al. Experimental study of the facial artery: relevance to its reverse flow competence and cutaneous blood supply of the neck for clinical use as a new flap. *Head Neck* 1996;18:17–23
29. Ramkumar A, Francis NJ, Kumar RS. Bipaddled submental artery flap. *Int J Oral Maxillofac Surg* 2012;41:458–460

OPEN

Preliminary Study on Composition and Microstructure of Calcification in Craniopharyngiomas

Junxiang Peng, MD, Songtao Qi, MD, PhD,* Jun Pan, MD, PhD,* Xi'an Zhang, MD, PhD,* Guanglong Huang, MD,* and Danling Li, MD†*

Abstract: To analyze the element composition and microstructure of calcification in craniopharyngiomas and to explore the differences among differing degrees of calcification, 50 consecutive

patients with craniopharyngioma were selected. X-ray diffraction analysis and energy-dispersive X-ray spectroscopy analysis were performed on the calcified plaques isolated from the tumor specimens. All calcified plaques were constituted of hydroxyapatite crystals and some amorphous materials. The main elements for the analysis were calcium, phosphate, carbon, and oxygen. There were significant differences among groups of differing degrees of calcification in the percentage composition of calcium, phosphorus, and carbon ($P < 0.05$), in which the element content of calcium and phosphorus had a positive correlation with the extent of calcification (rp = 0.745 and 0.778, respectively, $P < 0.01$), while the element content of carbon had a negative correlation with the extent of calcification (rp = −0.526, P <0.01). The calcium, phosphorus, and carbon content are different in calcified plaques with different extents of calcification. The element content of calcium, phosphorus, and carbon influences the degree of calcification.

Key Words: Calcification, composition, craniopharyngiomas, microstructure

Craniopharyngioma (CP) is one of the most commonly calcified tumors of the central nervous system. The calcification patterns vary from solid lumps to popcorn-like foci or less commonly to an eggshell pattern lining the cyst wall.[1–3] However, the molecular mechanisms that result in calcification of CP are unclear.[4,5]

The element composition and microstructure of a certain substance determines the physicochemical macroscopic properties of the substance, including shape, texture, hardness, solubility, melting point, etc. So it is conferred that different types of calcification will exhibit a wide diversity in texture, appearance, radiologic findings, and clinical features, which is probably caused by the difference in the microcosmic composition.[6–9]

In this study, we used X-ray diffraction analysis and energy-dispersive X-ray spectroscopy analysis techniques to perform an exploratory study on the element composition and phases of calcification in craniopharyngiomas to understand fully the nature of calcification in craniopharyngiomas at the micro level. Based on test data analysis, specimens of different extents of calcification were compared between groups to explain the features of calcification in craniopharyngiomas and make some preliminary discussion on the possible formation mechanism and some new ideas about the treatment of calcification in craniopharyngiomas.

From the *Department of Neurosurgery, Nanfang Hospital, Southern Medical University; and †Biological Statistics Department, School of Public Healthy and Tropical Medicine, Southern Medical University, Guangzhou, Guangdong, China.

Received February 9, 2016.
Accepted for publication March 13, 2016.

Address correspondence and reprint requests to Songtao Qi MD, PhD, Danling Li, MD, Department of Neurosurgery, Nanfang Hospital, Southern Medical University, Guangzhou 510515, Guangdong, China; E-mail: sjwkqisongtao@126.com; sjwkmarco@126.com

This research received grant from 4 fund projects in the public, including the National Natural Science Foundation of China (No. 81402759), Guangdong province medical fund (A2015076) and President Foundation of Nanfang Hospital, Southern Medical University (No. 2014B020).
The authors report no conflicts of interest.

ISSN: 1049-2275
DOI: 10.1097/SCS.0000000000002676

METHODS

Surgical calcified specimens from 50 patients with CP were retrieved from the archives of the Department of Neurosurgery at the Nangfang Hospital, Southern Medical University, from January 2008 to March 2012. This group included 29 males ranging in age from 3 to 66 years (mean, 21.3 ± 3.1) and 21 females ranging in age from 3 to 55 years (mean, 24.0 ± 3.4). Fresh specimens were obtained immediately following surgical resection in all patients. The powdered samples from calcified specimens were not less than 0.15 mL to satisfy the minimum requirements for testing instruments.

In all patients, axial noncontrast and contrast-enhanced computed tomographic scans with a section thickness varying from 2 to 4 mm were obtained. Additionally, the clinical recording of the CP was obtained in all of the patients.

Calcification in craniopharyngiomas was graded into 3 categories according to the size on computed tomographic images (grade 1 = sandlike or scattered, punctate calcification [+]; grade 2 = eggshell calcification [++]; grade 3 = massive calcification with a diameter greater than 5 mm [+++]) (Fig. 1).

SPECIMEN PROCESSING

Specimens were obtained fresh from the operating room and calcifications were isolated immediately under the operating microscope. Blood and craniopharyngioma cyst fluid were washed with double-distilled water. The specimens were soaked in distilled water for 72 hours, so that small amounts of tissue attached to the calcifications would naturally decay and fall off. After immersion, the specimens were taken out and thoroughly washed with double-distilled water, and then air dried for 24 hours. Based on the requirements for X-ray crystallographic powder diffraction, the specimens were ground to a fine powder in an agate mortar. The required particle size of the samples was approximately 10 μm with a smooth feel like flour. The ground specimens were placed in a glass desiccator at room temperature overnight and the samples were fully dried, then examined. Frozen specimens were thawed at room temperature. The following specimen processing methods were the same as those of the fresh specimens.

DETECTION METHODS AND INDEXES

X-Ray Diffraction Analysis

Samples were evenly spread over a monocrystalline silicon wafer and mounted on the sample platform of a D8 Advance

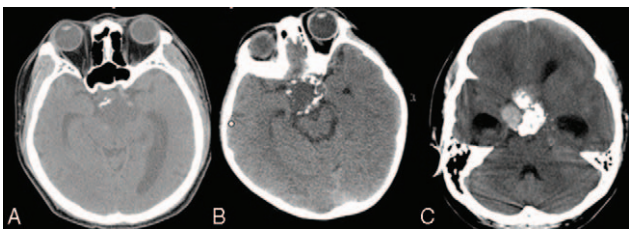

FIGURE 1. Computed tomography scan show calcification in craniopharyngiomas. (A) Cystic CP with solid lump calcification (+). (B) Cystic CP with calcium in the cyst wall as eggshell pattern (++). (C) Intrasellar and suprasellar tumor with popcorn-like foci (+++). CP. craniopharyngioma.

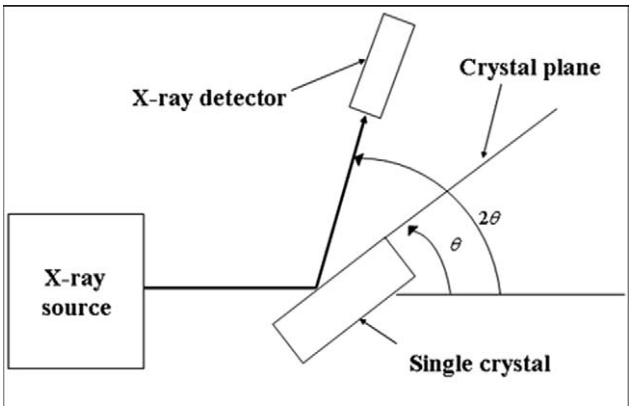

FIGURE 2. Schematic diagram of crystal diffraction.

X-ray diffractometer. Combinations of the following working parameters were analyzed: start angle 8.000°, stop angle 60.000°, with a scanning step of 0.020° at a generator voltage of 40 kV and generator current of 40 mA. A Bruker automatic powder X-ray diffractometer (D8 Advance) was used to record diffraction patterns. The powder diffraction pattern was obtained using TOPAS software suites. The diffraction peak was measured manually and marked. By using the software, the relevant parameter *d* value (the interplanar spacing of crystal plane) could be automatically calculated. Based on the known parameters grazing angle θ (the grazing angle of the incident X-ray and reflection of the crystal plane, shown in Fig. 2), the wavelength λ (the wavelength of the incident X-ray), and calculated *d* value, retrieval was carried out in the powder diffraction card (PDF card) to determine the crystal phase composition.

X-Ray Energy-Dispersive Spectroscopy Analysis

Energy disperse spectroscopy worked combined with scanning electron microscopy. Samples were bombarded with electrons generated by scanning electron microscopy. The calcification samples obtained via X-ray diffraction analysis were recovered and placed onto the stage of a scanning electron microscope. Samples were spread evenly and fixed with special glue, then put into the sample compartment of scanning electron microscope. For the small sample amount, samples were not treated by spray-gold but admitted directly to the low vacuum for detection. The parameters of scanning electron microscope were set as follows: 500 k × magnification with a 20 kV operating voltage. The X-Flash detector of the spectrometer was set and K transition photon was selected. Electro beam scanning was performed at regions with evenly distributed samples at ×500 magnification and detector received transition photon. Data analysis and processing were done by its own quantitative analysis software without standards. The results obtained were element species and their percentage in the sample.

Statistical Analysis

Data were expressed as mean ± standard deviation and analyzed by statistical software SPSS13.0. One-way analysis of variance was applied in the percentage composition of calcium, phosphorus, and carbon among groups of differing degrees of calcification. Bivariate correlation analysis was used to analyze the relationship between percentage composition of elements, percentage composition of elements, and differing degrees of calcification. A one-sample *t* test was used to compare the actual calcium/phosphorus ratio with the theoretical values. All tests of statistical significance were two-tailed; alpha was set at 0.05. A *P* value of 0.05 was considered statistically significant.

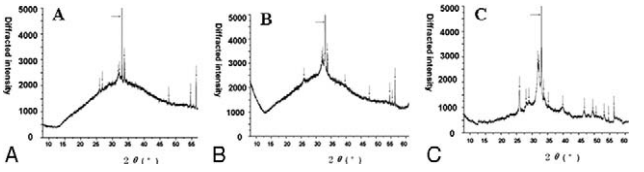

FIGURE 3. Diffraction of different degree calcification samples: (A) (+); (B) (++); (C) (+++) → show the characteristic diffraction peaks of monocrystalline silicon back, ↓shows the diffraction peaks of hydroxyapatite.

RESULTS

Analysis Results of X-Ray Diffraction

Of the 50 calcified specimens, the crystalline material was hydroxyapatite with the chemical formula Ca10 (PO4)6(OH)2 and the molecular weight of 1 004. No samples were pure hydroxyapatite crystals and they were mixed with amorphous material to varying degrees. The X-ray diffraction chart of the sample was displayed that when the value of 2θ ranged from 32.97° to 33.09°, there was a corresponding extremely sharp diffraction peak that was the characteristic diffraction peak of monocrystalline silicon (used as diffraction background or positive control). The remaining diffraction peaks marked were identified the diffraction peaks of hydroxyapatite after software analysis (Fig. 3).

Analysis Results of X-Ray Energy-Dispersive Spectroscopy

The element contents of all calcified specimens were calcium, phosphorus, carbon, and oxygen as well as a small amount of sodium and magnesium. Some specimens contained a trace of 1 or several sorts of potassium, chlorine, aluminum, silicon, ferrum and sulfur (with percentage composition less than 0.5%). A trace of chromium was measured in 2 calcified specimens. The percentage content of calcium, phosphorus, and carbon in grade 1, grade 2, and grade 3 existed significant differences ($P < 0.05$) (Fig. 4).

The element content of calcium and phosphorus had a positive correlation with the extent of calcification ($r\text{p} = 0.745$ and 0.778, respectively, $P < 0.01$), while the element content of carbon had a negative correlation with the extent of calcification ($r\text{p} = -0.526$, $P < 0.01$). The element content of calcium had a positive correlation with that of the phosphorus ($r\text{p} = 0.938$, $P < 0.001$), while the element content of calcium and phosphorus had a negative correlation with that of the carbon ($r\text{p} = -0.844$ and -0.786, respectively, $P < 0.01$) (Fig. 5).

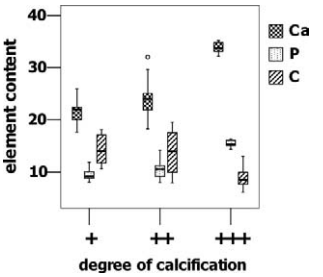

FIGURE 4. A comparison between different levels of calcium and phosphorus and carbon content of calcification. $P < 0.05$.

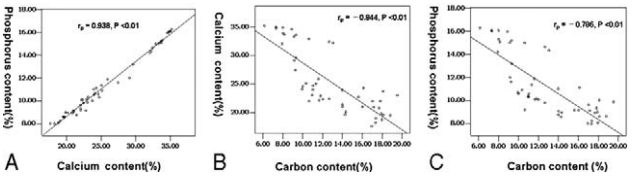

FIGURE 5. Scatter diagram shows relationship between calcium, phosphorus, carbon. (A) The element content of calcium had a positive correlation with that of the phosphorus. (B) The element content of carbon had a negative correlation with the extent of calcification. (C) The element content of calcium and phosphorus had a negative correlation with that of the carbon.

DISCUSSION

Clinical observations showed that grade 1 calcification was soft or loose in texture, gray in color and rarely, or to a lesser extent adhered to the adjacent organs such as hypothalamus, mammillary bodies. However, grade 3 calcification was hard, white in color, some even with a metallic luster, adhered more closely to the adjacent organs. So we believe that it is easier to dissect grade 1 and grade 2 calcifications than grade 3 calcification intraoperatively and sometimes part of the residual mass remained.

The texture, shape, imaging findings, and even clinical manifestations of calcification in craniopharyngiomas are not the same, indicating that there are differences among different grades of calcification. The element composition and microstructure of a certain substance determine the physicochemical macroscopic properties of the substance. Therefore, we believe that there exist differences in the microcosmic composition of different grades of calcification. We used X-ray diffraction analysis and energy-dispersive X-ray spectroscopy analysis techniques to perform a microanalysis for different grades calcification to understand their differences at the micro level. Diffraction from crystalline materials follows Bragg law: $2d\sin\theta = n\lambda$.[10,11]

When the interplanar crystal spacing d is known, according to Bragg law, diffraction can be generated only in X-ray incidence angle θ to the crystal surface (see Fig. 2). Therefore, the chart of X-ray diffraction patterns strictly corresponds to the crystal structure and the characteristic diffraction patterns of each crystal will not change with the mixture of different crystal materials. Based on this feature, powder diffraction of polycrystalline materials can identify different crystal components, which requires a sufficiently large number of small grains.[3] There are certain requirements for the amount of powder sample (The experimental equipment used in this study requires not less than 0.15 mL of sample amount). With large size of grade 3 calcified plaque, it can provide sufficient sample size, while it is more difficult to collect enough sample size of grade 1 calcified plaque because of its small size and scattered distribution. So radical resection should be advocated for craniopharyngiomas.[12–14] The majority of craniopharyngiomas can be completely removed, thus ensuring grade 1 calcified plaque for a sufficient sample size, to meet the equipment requirements.

The study also found that the baselines of the X-ray diffraction diagram taken from all samples increased by varying degrees and were jagged in shape, which were significantly different from those of the diffraction diagram from pure crystal component. The elevated baselines represented the amount of amorphous materials the sample contained. Generally speaking, the higher the baseline sample was, the lower the degree of crystallinity and the higher the content of amorphous materials would be. In addition, the diffraction peak of hydroxyapatite in specimens tended to become broad to various degrees. According to the principle of crystal diffraction,[7] it could be speculated that there existed lattice distortions in hydroxyapatite specimen, which meant that symmetric spatial structure under an ideal state lost in some crystal cells. The higher the proportion of the distorted crystal cells, the lower the crystallinity of the crystal. Energy spectrum analysis in this study showed that the calcified plaques in craniopharyngiomas mainly contain 4 elements (calcium, phosphorus, carbon, and oxygen), which is in accordance with Azari results.[14] It was assumed that calcified plaques only contained hydroxyapatite crystal composition, so the element species in the sample should only be calcium, phosphorus, oxygen, and hydrogen (for hydrogen atom mass was too light to detect with energy spectrometer currently) without carbon. Even there was a small amount of carbon-containing compound contaminated, the percentage content of carbon was rather low. The theoretical value was calculated in accordance with the molecular formula and molecular weight of hydroxyapatite with percentage content of calcium and phosphorus and calcium/phosphorus ratio 39.8%, 18.5%, and 2.15, respectively. The percentage content of carbon in the study was second only to that of oxygen and calcium with an average percentage of $(12.79 \pm 3.76)\%$, which could not be explained by contamination. The percentage content of the corresponding calcium and phosphorus was lower than the theoretical value.

Combined with X-ray diffraction analysis, we believe that carbon originated from amorphous material in the specimens. In this study, the actual measured calcium/phosphorus ratio was 2.60 ± 0.21, which was significantly different (1-sample t test, $P < 0.001$) compared with the theoretical value (2.15). The results suggested that the phosphorus content of all samples was less than the theoretical content required for the formation of hydroxyapatite crystals, which probably because of phosphate deficiency or the replacement of phosphate by other atoms or atomic groups during the growth process of hydroxyapatite crystal. One of the results was lattice distortion, thus leading to decreased crystallinity.

In conclusion, the calcification in craniopharyngiomas was different at microlevel (including the element composition and microstructure) according to the calcification grade. The element content of calcium, phosphorus, and carbon influences the degree of calcification. Samples with high calcium and phosphorus content and low carbon content have high degree of calcification. And samples with low calcium and phosphorus content and high carbon content have low degree of calcification. It has been reported that the formation of hydroxyapatite would be significantly affected when the ion concentration changed.[6] So we speculate that if the ionic microenvironment of calcified plaque in craniopharyngiomas is changed, the degree of calcification will decrease. If the above goal is achieved, it can reduce the degree of difficulty in surgery of grade 3 calcified craniopharyngiomas as well as the risk of injury to adjacent organs.

ACKNOWLEDGMENTS

The authors thank Fan Jun, MD, Qiu Xiao-Yu, RN, Mo Yi-Ping, RN, and Shi Jing, BA, for the collection of data and care of patients enrolled in this study.

REFERENCES

1. Qi S, Huang G, Pan J, et al. Involvement of osteopontin as a core protein in craniopharyngioma calcification formation. *J Neurooncol* 2010;98:21–30
2. Lee MH, Kim SH, Seoul HJ, et al. Impact of maximal safe resection on the clinical outcome of adults with craniopharyngiomas. *J Clin Neurosci* 2012;19:1005–1008
3. Wisoff JH. Craniopharyngioma. *J Neurosurg Pediatr* 2008;1:124–125
4. Hussain I, Eloy JA, Carmel PW, et al. Molecular oncogenesis of craniopharyngioma: current and future strategies for the development of targeted therapies. *J Neurosurg* 2013;119:106–112

5. Donley GE, Fitzpatrick LA. Noncollagenous matrix proteins controlling mineralization; possible role in pathologic calcification of vascular tissue. *Trends Cardiovasc Med* 1998;8:199–206
6. Azari F, Vali H, Guerquin-Kern JL, et al. Intracellular precipitation of hydroxyapatite mineral and implications for pathologic calcification. *J Struct Biol* 2008;162:468–479
7. Sun Y, Zeng XR, Wenger L, et al. Basic calcium phosphate crystals stimulate the endocytotic activity of cells-inhibition by anti-calcification agents. *Biochem Biophys Res Commun* 2003;312:1053–1059
8. Giachelli CM. Inducers and inhibitors of biomineralization: lessons from pathological calcification. *Orthod Craniofac Res* 2005;8:229–231
9. Giachelli CM. Ectopic calcification: gathering hard facts about soft tissue mineralization. *Am J Pathol* 1999;154:671–675
10. Kopylov AM. X-ray analysis of ribosomes: the static of the dynamic. *Biochemistry (Mosc)* 2002;67:372–382
11. Shi X-E, Wu B, Fan T, et al. Craniopharyngioma: surgical experience of 309 cases in China. *Clin Neurol Neurosurg* 2008;110:151–159
12. Fahlbusch R, Honegger J, Paulus W, et al. Surgical treatment of craniopharyngiomas: experience with 168 patients. *J Neurosurg* 1999;90:237–250
13. John M, Duff, Fredric B, et al. Craniopharyngioma: the Mayo experience with 121 cases. *J Clin Neurol Neurosurg* 1997;99:S89
14. Azari F, Vali H, Guerquin-Kern JL, et al. Intracellular precipitation of hydroxyapatite mineral and implications for pathologic calcification. *J Struct Biol* 2008;162:468–479

The Complication of Middle Facelift Surgery Resulting in Migration of Temporal Augmentation Implant

Hwan Jun Choi, MD, PhD[*†] *and Jun Beom Lee, MD*[*]

Abstract: A 66-year-old woman admitted with induration, peri-wound marceration, swelling, and tenderness on temporal area. She had repeated painful tenderness on temporal area for 10 days. In the peri-wound, discharge volume increased when she ate spicy food or drank lemon juice. She had no trauma history and special medical history. But 3 weeks ago, she had midface lift surgery at another local clinic. Initially, the authors had aspiration to swelling spot, checked 50 cc serotic discharge. The authors checked contrast enhance facial computed tomography and found homogenous fluid collection and peripheral enhancing low attenuated lesion in the anterior portion of tragus and inferior aspect of left ear lobe. Also migration of ipsilateral temporal augmentation implant was shown as a result of seroma in temporal fossa. The authors decided to proceed with the surgical removal and diversion of fluid collection. Under local anesthesia, the authors had incision and drainage, inserted drainage tube and bag. After inserting a drainage device, daily discharge was reduced and the condition was treated conservatively with additional drainage and resolved completely in 3 weeks. There were no wound problems such as infection, disruption, and so on.

From the *Department of Plastic and Reconstructive Surgery, College of Medicine; and †Institute of Tissue Regeneration, Soonchunhyang University, Cheonan, Korea.

Received February 9, 2016.
Accepted for publication March 13, 2016.

Address correspondence and reprint requests to Hwan Jun Choi, MD, PhD, Department of Plastic and Reconstructive Surgery, Soonchunhyang University Cheonan Hospital, 23-20, Byeongmyeong-dong, Dongnam-gu, Cheonan-si, Chuncheongnam-do 330-721, Korea;
E-mail: medi619@hanmail.net

This work was supported by the Soonchunhyang University Research Fund.
The authors report no conflicts of interest.

ISSN: 1049-2275
DOI: 10.1097/SCS.0000000000002682

Key Words: Complication, midface lift, migration, parotid gland injury, temporal implant

With the development of science and medicine, the human life span has become much longer, and the demands for antiaging surgery have grown. Unlike general aesthetic plastic surgery, which addresses unaesthetic congenital qualities, antiaging surgery focuses on recovering the patient's youthful appearance that has faded away with age. When seen close up, wrinkles are the major cause of appearing old, while from far away, volume loss and drooping of tissues are the major causes of appearing old, and facelift is the most effective method to pull these tissues back upward. But facelift had some complication. Hematoma and seroma are most common complication after facelift, occurring in 1% to 8% of the patient. In rare patients, a parotid gland injury and skin necrosis and asymmetry are surgical complication known to occur following facelift surgery.

A 66-year-old woman admitted with induration, peri-wound marceration, swelling, and tenderness on temporal area. She had repeated painful tenderness on temporal area for 10 days. In the peri-wound, discharge volume increased when she ate spicy food or drank lemon juice. She had no trauma history and special medical history. But 3 weeks ago, she had midface lift surgery at another local clinic. Initially, the authors had aspiration to swelling spot, checked 50 cc serotic discharge. The authors checked contrast enhance facial computed tomography and found homogenous fluid collection and peripheral enhancing low attenuated lesion in the anterior portion of tragus and inferior aspect of left ear lobe. Also migration of ipsilateral temporal augmentation implant was shown as a result of seroma in temporal fossa. The authors decided to proceed with the surgical removal and diversion of fluid collection. Under local anesthesia, the authors had incision and drainage, inserted drainage tube and bag. After inserting a drainage device, daily discharge was reduced and the condition was treated conservatively with additional drainage and resolved completely in 3 weeks. There were no wound problems such as infection, disruption, and so on (Fig. 1).

Face volume loss and drooping of tissues are the major causes of appearing old and a facelift is the most effective method to pull these issues back upward. But face lifting had some complications, hematoma, seroma, and so on. An iatrogenic parotid gland injury can complicate other surgical procedures, such as facelift surgery. If injury to the parotid gland is overlooked during surgery, swelling is seen 5 to 7 days postoperatively, which increases when eating or can even create a fistula. Moreover, the symptoms of parotid injury can also develop after surgery. In the patient of ductal injuries, surgical intervention is the treatment principle, and in the patient of parenchymal injuries, conventional treatment may be sufficient to achieve correction in 4 to 5 weeks. In this patient, the authors can know parotid gland injury can occur by facelift surgery and augmentation implant migration can occur by seroma and inflammation of temporal fossa and mid or upper facial areas.

A parotid fistula and an accessory parotid gland abscess are surgical complications known to occur following parotid gland surgery[1] but have also been reported after other operations, such as